# Magnetocaloric properties and specifics of the hysteresis at the first-order metamagnetic transition in Ni-doped FeRh

A. M. Chirkova,[1,2] K. P. Skokov,[1] Y. Skourski,[3] F. Scheibel,[1] A. Y. Karpenkov,[4] A. S. Volegov,[5,6] N. V. Baranov,[5,6] K. Nielsch,[2,7] L. Schultz,[2,7] K.-H. Müller,[2] T. G. Woodcock,[2] and O. Gutfleisch[1]

[1]*TU Darmstadt, Institute for Materials Science, 64287 Darmstadt, Germany*
[2]*IFW Dresden, Institute for Metallic Materials, 01067 Dresden, Germany*
[3]*Dresden High Magnetic Field Laboratory, Helmholtz-Zentrum Dresden-Rossendorf, 01328 Dresden, Germany*
[4]*NUST "MISiS," 119049 Moscow, Russia*
[5]*Institute of Natural Sciences, Ural Federal University, Yekaterinburg 620083, Russia*
[6]*Institute of Metal Physics, Ural Branch of Russian Academy of Sciences, Yekaterinburg 620990, Russia*
[7]*TU Dresden, Institute of Materials Science, 01062 Dresden, Germany*

(Received 16 February 2021; accepted 19 May 2021; published 21 June 2021)

Measurements of the magnetization in quasistatic and pulsed magnetic fields with different sweep rates, measurements of the specific heat in various magnetic fields, and direct measurements of the adiabatic temperature change have been employed to study the metamagnetic phase transition from an antiferromagnetic (AF) to the ferromagnetic (FM) state in an $(Fe_{0.98}Ni_{0.02})_{49}Rh_{51}$ alloy with a critical AF-FM transition temperature, $T_{tr}$, reduced to 266 K. Based on the obtained results, a magnetic phase diagram for this alloy has been constructed. The AF-FM transition induced by the magnetic field below 10 K is found to occur in a steplike fashion in contrast to smooth behavior at $10\,\mathrm{K} < T < T_{tr}$. The adiabatic temperature change $\Delta T_{ad}$ in the magnetic field of 2 T exceeds 6.5 K in pulsed fields (∼100 T/s) and in the Halbach setup (∼0.5 T/s), which is in agreement with the estimation from the *S*-*T* diagram constructed based on the specific heat measurements. The reversible $\Delta T_{ad}$ reaches −4.6 K under cyclic conditions in the Halbach setup (2 T). A complete transformation to the FM state in the whole temperature range requires a magnetic field of 14 T. Direct measurements of $\Delta T_{ad}$ in pulsed fields of 14 T revealed an irreversible part of the magnetocaloric effect associated with the presence of magnetic hysteresis and respective losses during the magnetization process.

DOI: 10.1103/PhysRevMaterials.5.064412

## I. INTRODUCTION

Materials with magnetostructural phase transitions are a key component of the magnetic refrigeration technology—an environmentally friendly alternative to conventional cooling [1,2]. The success of this technology requires both progress in the development of materials suitable as magnetic refrigerants [3,4] and in the engineering of cooling devices [5]. Significant progress has been made over the past 20 years after the report of a giant magnetocaloric effect (MCE) in $Gd_5Si_2Ge_2$ [6], which triggered intense research of materials with first-order transitions. The refrigerants commonly considered for use in prototypes that combine both efficiency and low cost are represented by iron- and manganese-based material families, such as $La(Fe_{1-x}Si_x)_{13}$, Heusler alloys, and FeMn(As,P) [7–9]. However, the most efficient room-temperature magnetic refrigerant is still Gd, which has an adiabatic temperature change $\Delta T_{ad}$ of about 5 K in a 2 T field at the second-order ferromagnetic-paramagnetic transition. Materials with first-order magnetic phase transitions typically exhibit a higher MCE in the magnetic field of 1–2 T, but the transformation is accompanied by hysteresis, which leads to a reduction of the MCE in a real magnetic refrigeration cycle [10,11]. For such materials, experiments under cyclic conditions are required [12]. The thermal hysteresis in magnetocaloric materials can be tuned by different ways [13]. Studies of intrinsic (e.g., chemical order, coupling of sublattices, electronic structure, etc.) and extrinsic aspects (e.g., microstructure, kinetics, defects, etc.) are vitally important for better understanding of the hysteretic phenomena in magnetocaloric materials and for future applications [14]. Furthermore, at a first-order transition via the nucleation and growth process, the system passes through a state where both new and parent phases coexist; hence the kinetics of the transformation becomes an important point as well [15,16].

Among the materials with the first-order magnetic phase transitions, FeRh exhibits a giant MCE that had been reported even earlier than in $Gd_5Si_2Ge_2$ and remains the largest in a 2 T field near room temperature [17,18]. Under cyclic conditions the reversible value of $|\Delta T_{ad}|$ is about 6 K, which is higher than in Gd in the same magnetic field, as has been demonstrated for the binary compound [19,20]. Despite the cost of raw materials, FeRh remains a suitable and fascinating model system for fundamental magnetocaloric studies. The data on $\Delta T_{ad}$ of FeRh and related compounds modified by other *d* elements are still scarce. This information is, however, relevant for the understanding of the magnetocaloric materials, as doping is often used to tailor the transition

 

temperature towards a particular temperature range [21,22]. Moreover, due to the critical field dependence on temperature [23], the equiatomic $Fe_{50}Rh_{50}$ with the antiferromagnetic (AF)-ferromagnetic (FM) transition temperature close to 400 K in zero magnetic field would require a magnetic field of about 40 T to induce the transition in the whole range down to low temperatures.

It is known that the temperature of the transition in FeRh is sensitive to the magnitude of an applied magnetic field or stress, as well as to the change of stoichiometry within the binary system or substitution by other *d* elements [24]. For example, a substitution of Ni for Fe allows the transition to be tuned towards lower temperatures [22]. For this work, we have chosen a sample of $Fe_{49}Rh_{51}$ doped with 1 at. % Ni with the AF-FM transition at $T_{tr} = 266$ K in zero field, and a maximal required field of 14 T to induce the transition at low temperature. That allowed us to investigate the metamagnetic transition in FeRh, magnetocaloric properties, and specifics of its hysteretic behavior in a broad temperature range under adiabatic and isothermal conditions applying different magnetic field sweep rates.

## II. EXPERIMENT

The sample of $(Fe_{0.98}Ni_{0.02})_{49}Rh_{51}$ composition was prepared by arc melting of pure elements Fe (99.98%), Ni (99.99%), and Rh (99.8%) in helium atmosphere in a water-cooled Cu crucible; the homogenizing heat treatment was done in an evacuated quartz ampoule for 10 days at 1000 °C followed by quenching. The x-ray diffraction (XRD) characterization was done in a Bruker D8 Advance diffractometer with Co radiation; the microstructure and local phase composition were investigated by a scanning electron microscope JEOL JSM-6510 equipped with a Bruker EDS system. The sample consists mainly of the CsCl-type ($\alpha'$) phase with the lattice parameter $a = 0.2997$ nm and a small amount (6 vol %) of the paramagnetic fcc ($\gamma$) phase with the lattice parameter $a = 0.3766$ nm (see Fig. 1 in the Supplemental Material [25]). The amount of the minor phase is higher compared to the binary alloy [26]. The lattice parameter of the main phase is larger than that of the binary alloy; however, this is mainly due to a different magnetic state at room temperature. The binary alloys investigated earlier [26] were all in the AF state at room temperature, while this Ni-doped alloy has a lower transition temperature and therefore is already in the FM state that is characterized by 1% higher volume of the unit cell.

Magnetization measurements were carried out in a Quantum Design physical property measurement system (PPMS) 14 T in magnetic fields up to 14 T with a field sweep rate of 0.005 T/s. Additionally, magnetic measurements were done at four selected temperatures with the sweeping rate of $10^2$–$10^3$ T/s using a pulsed magnetic field in the Dresden High Magnetic field laboratory (HLD) at the Helmholtz-Zentrum Dresden-Rossendorf (HZDR) [27]. The heat capacity in magnetic fields of 0, 1.9, and 14 T was measured using a Quantum Design (PPMS) 14 T. For the indirect evaluation of the magnetic entropy change at the AF-FM transition, temperature dependences of the magnetization $M(T)$ were measured in a Quantum Design magnetic property measurement system (MPMS) on heating and cooling with a step size of 0.2 T.

Direct measurements of the adiabatic temperature change $\Delta T_{ad}$ were carried out in an experimental setup based on two nested Halbach cylinders with a uniform magnetic field directed perpendicular to cylinder axes. Mutual rotation of the cylinders resulted in a harmonically varying magnetic field of $\pm 1.93$ T. The frequency used in the experiment was $\frac{1}{18}$ Hz, which corresponds to a maximum field sweep rate of 0.5 T/s. The setup is described in detail elsewhere [10,15]. Alternatively, direct measurements of $\Delta T_{ad}$ were also done in pulsed fields with a rate of $10^2 - 10^3$ T/s in an experimental setup [28] at HLD HZDR [27]. In both cases, the temperature change of the sample was monitored with a copper-constantan thermocouple attached to the sample. In the Halbach setup, the direct measurements were carried out in the discontinuous mode, as well as under cyclic conditions (described in [19]), and in pulsed fields only in the discontinuous mode. In the discontinuous mode, every measurement starts from the same initial state achieved by (i) zero field cooling beyond the transition region and (ii) heating up to the target temperature, whereas measurements under cyclic conditions in the reapplied magnetic field reveal the behavior of the material in a real cooling cycle. The direct measurements of $\Delta T_{ad}$ were carried out using two plates with the approximate size of 5 mm × 4 mm × 1.5 mm forming a sandwich that clamps the thermocouple. Smaller pieces of a rectangular shape with the dimensions of 4 mm × 1.5 mm × 0.8 mm cut from the same ingot were used for magnetic measurements in pulsed and dc fields, as well as for the heat capacity measurements.

## III. RESULTS AND DISCUSSION

### A. Magnetocaloric effect in magnetic fields of 2 and 14 T

The indirect estimation of the MCE at the AF-FM transition has been done from the temperature dependences of magnetization and specific heat. Specific heat measurements were carried out in the temperature range of 2–390 K in 0, 1.9, and 14 T magnetic field (Fig. 1). The AF-FM transition in zero

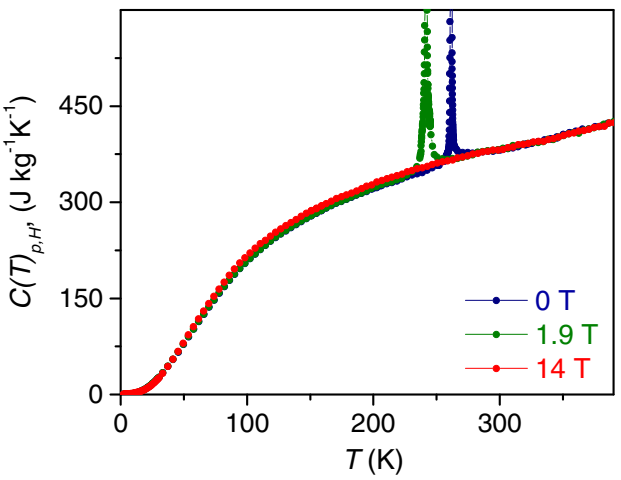


FIG. 1. Temperature dependences of the specific heat of $(Fe_{0.98}Ni_{0.02})_{49}Rh_{51}$ measured on heating in zero field (blue), in 1.9 T (green), and in 14 T (red).

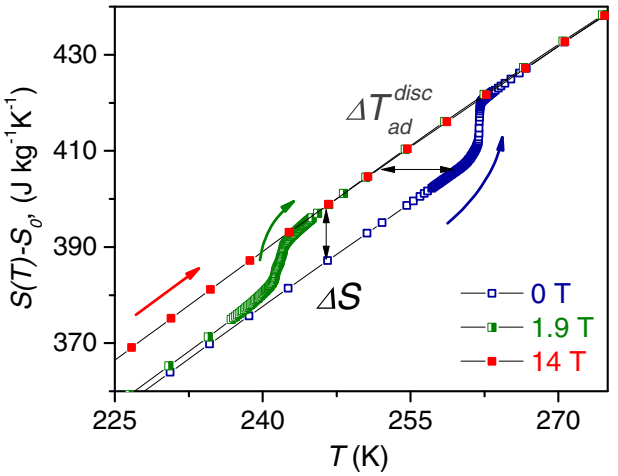


FIG. 2. *S-T* diagram obtained by the integration of the specific heat data in different magnetic fields.

field occurs at 266.5 K (on heating). Integrating the obtained dependences by $S(T)_H = \int_0^T [C_H(T)/T]dT$, an *S-T* diagram was constructed (Fig. 2). This allows, in the next step, both the entropy change and adiabatic temperature change in the respective magnetic fields to be estimated, as shown in Fig. 2 by black arrows.

Temperature dependences of magnetization $M(T)$ were measured in the range of AF-FM transition on heating and on cooling in fields from 0.2 to 2 T [Fig. 3(a), only heating curves are shown]. The evaluation of the entropy change was performed using Maxwell relations $\Delta S(T)_{\Delta H} = \int_{H_I}^{H_F} \frac{\partial M(T,H)}{\partial T} dH$ [29]. The respective $\Delta S(T)$ in different fields are given in Fig. 3(b). From $M(T)$ dependences one can estimate, for this temperature range, the shift of the transition temperature with magnetic field $dT/dH = -11\,\mathrm{K/T}$ and the change in magnetization at the transition $\Delta M = 127\,\mathrm{A\,m^2/kg}$. Therefore, applying the Clausius-Clapeyron equation, the maximal entropy change can be found as $\Delta S = 11.5\,\mathrm{J/(kg\,K)}$. The estimation from Maxwell relations gives a smaller number $\Delta S = 10.3\,\mathrm{J/(kg\,K)}$, as in the case of binary FeRh [19]. Using the estimated maximal values of the entropy change $\Delta S = 10.3 - 11.5\,\mathrm{J/(kg\,K)}$ and the specific heat before the transition $C_0 = 367\,\mathrm{J/(kg\,K)}$, the maximal expected adiabatic temperature change at the AF-FM transition, according to $\Delta T_{ad,\max} = (T_{tr}/C_0)\Delta S_{\max}$, should be $\Delta T_{ad,\max} = 7.5 - 8.3\,\mathrm{K}$.

The $\Delta S(T)$ plots in Fig. 3(b) are valid for the complete AF-FM transformation from the pure AF state without accounting for the hysteresis. However, using $\Delta S(T)$ dependence obtained from isofield $M(T)$ on both heating and cooling, one can estimate the region where the MCE is expected to be reversible [30]. This has been done here for the 2T field; the result is shown in Fig. 4 as a shaded area. Also, in Fig. 4, $\Delta S(T)$ the 2 T field calculated from the Maxwell relations is compared to $\Delta S(T)$ estimated from the *S-T* diagram: they are in very good agreement. Compared to the binary FeRh compound reported earlier in a similar study [19], in this Ni-doped FeRh, the maximal value of the entropy change is about 20% lower; however, the temperature region where the material should exhibit high values of $\Delta S$ under reapplied

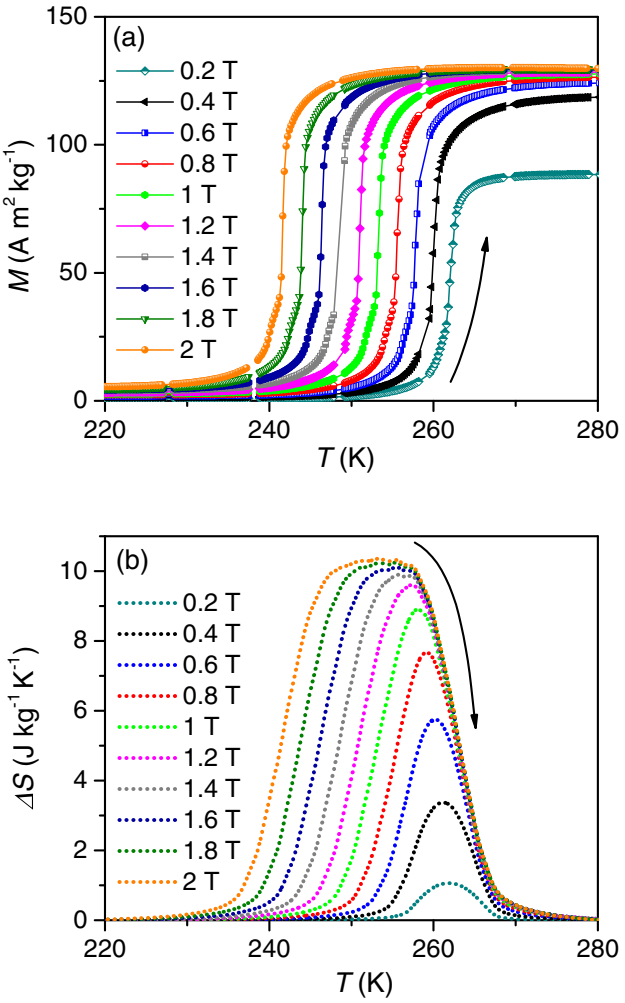


FIG. 3. (a) Temperature dependences $M(T)$ of the magnetization of $(Fe_{0.98}Ni_{0.02})_{49}Rh_{51}$ in static magnetic fields up to 2 T and (b) entropy change calculated from $M(T)$ using the Maxwell relations.

field is two times broader and extends over 20 K from 236 to 256 K compared to a 10 K range (309–316 K) in $Fe_{49}Rh_{51}$.

The direct measurements of the adiabatic temperature change $\Delta T_{ad}$ have been carried out using two different sources of magnetic field: Halbach setup (field sweep rate 0.5 T/s and maximal field 1.93 T) and pulsed field (field sweep rates of 140 and 1000 T/s on the field increase up to 2 and 14 T, respectively). The temperature dependence of $\Delta T_{ad}$ in the 2 T magnetic field obtained in the discontinuous mode at the first field application is plotted in Fig. 4 (circles and triangles) together with the indirect estimate from the *S-T* diagram. There is good agreement between the *S-T* diagram and the measurements in pulsed fields; however the absolute values in the Halbach setup are lower. The maximal discontinuous $\Delta T_{ad}$ in Ni-doped FeRh shows a 23% reduction compared to the binary sample [19]; however the cyclic value is reduced only by 12% and remains quite high ($\Delta T_{ad,\mathrm{cycl}} = -4.6\,\mathrm{K}$ in $\Delta\mu_0 H = 1.9\,\mathrm{T}$).

To answer the question of how the MCE in this sample behaves upon a further field increase, direct measurements in pulsed fields were carried out in a high magnetic field of 14 T. The results of the direct measurements are shown in

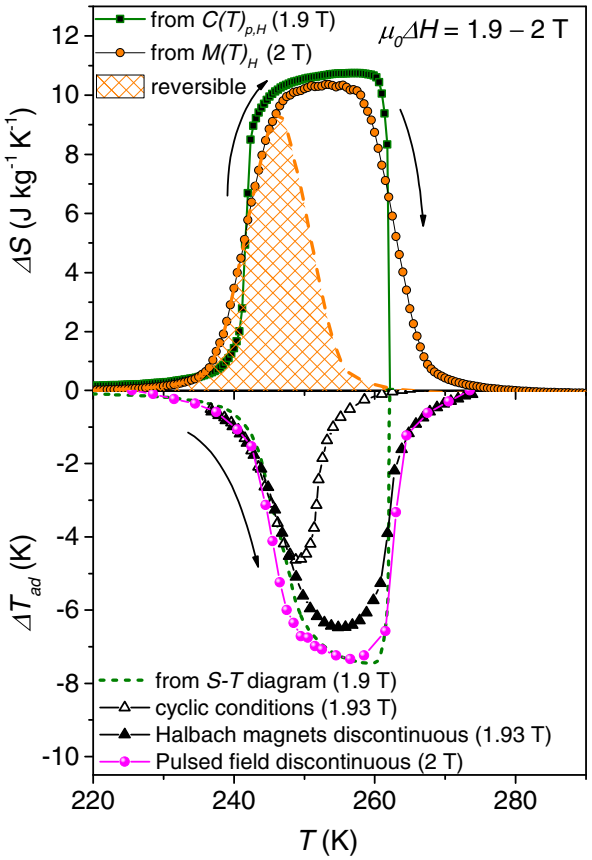


FIG. 4. Entropy change in a 2 T field estimated from Maxwell relations and the $S$-$T$ diagram. Shaded area shows the range of reversible MCE. Temperature dependences of the adiabatic temperature change obtained by direct measurements: in pulsed field (stars), direct measurements in Halbach setup (closed triangles), and estimated indirectly from the $S$-$T$ diagram (dashed line). Open triangles show $\Delta T_{ad}$ data obtained under cyclic conditions.

Fig. 5: For all four temperatures a full transformation is induced; $\Delta T_{ad}$ reaches saturation and does not increase further with field. In this experiment we do not observe the conventional magnetocaloric effect after the AF-FM transition as other authors have [31]. The adiabatic temperature change reaches the maximal value $|\Delta T_{ad}| = 7.1$ K during the measurement at 238 K, which is close to the transition temperature in zero field and $\Delta T_{ad}$ decreases towards lower temperatures. It is notable that the temperature of the sample after the pulse measurement is increased: This effect becomes stronger towards lower temperatures and reaches 1 K at 122 K. However, there is no evidence of such effect by direct measurements of $\Delta T_{ad}$ in other magnetocaloric materials, e.g., in La(Fe, Co, Si)$_{13}$ [32] or Heusler alloys [15]. The only similar behavior can be found at another AF-FM magnetostructural transition in $Mn_3GaC$ [16]. Therefore, this effect might be common for materials experiencing a magnetic phase transition of an order-order type without a change in crystal symmetry. We will address this effect also in the next section. The data on $\Delta T_{ad}$ in 2 and 14 T magnetic fields obtained by direct measurements and the indirect method are summarized in Fig. 6. The values estimated from the $S$-$T$ diagram are

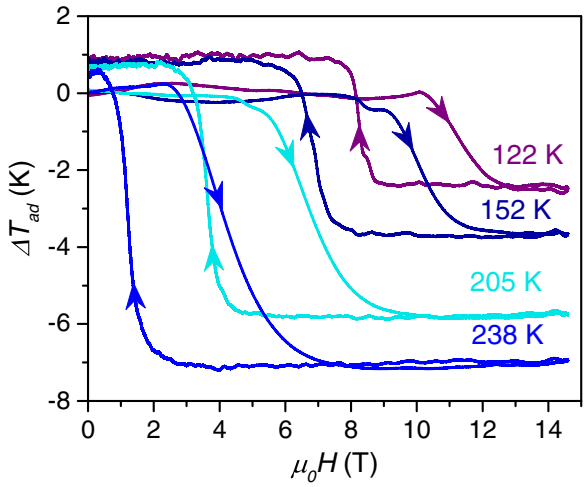


FIG. 5. Field dependences of $\Delta T_{ad}$ in $(Fe_{0.98}Ni_{0.02})_{49}Rh_{51}$ obtained by direct measurements in a pulsed field of 14 T.

shown as dashed lines, circles show the pulsed field data, and triangles are obtained by measurements in the Halbach setup; there is good agreement between all three methods. One can observe a linear variation of $\Delta T_{ad}$ with temperature in the high magnetic field (14 T).

### B. Magnetization measurements in quasistatic and pulsed fields

First, the temperature dependence of the magnetization for this alloy was explored using static magnetic fields up to 14 T (Fig. 7). The measurements in applied field were done on cooling and then on heating. The magnetic field of 14 T was sufficient to suppress the magnetostructural transition and retain the FM state down to low temperatures, as can be seen in Fig. 7. As the magnetic field increases, it stabilizes the FM state and reduces the transition temperature. It is noticeable that besides the broadening of the thermal hysteresis by the

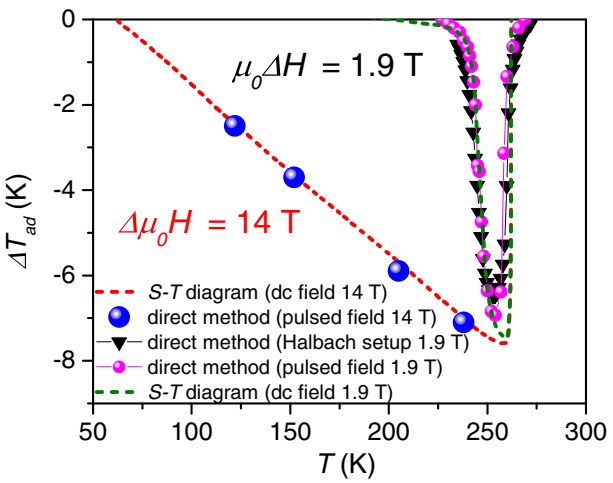


FIG. 6. Adiabatic temperature change for 2 and 14 T field measured directly in pulsed magnetic fields (circles) compared to the direct measurements in Halbach setup in 1.9 T (triangles) as well as to the values obtained from the $S$-$T$ diagram for 1.9 and 14 T (dashed lines).

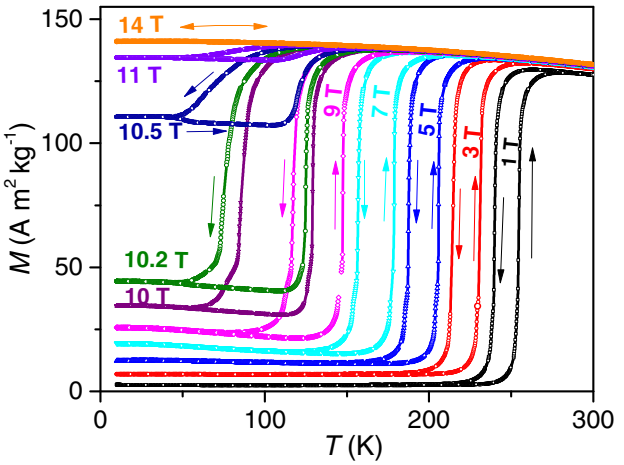


FIG. 7. Isofield temperature dependences of the magnetization of $(Fe_{0.98}Ni_{0.02})_{49}Rh_{51}$ measured on cooling and subsequent heating.

shift of the transition towards lower temperatures, there is an increasing amount of the low temperature FM contribution. At the magnetic field of 10 T and higher, the transition temperature on heating practically stops shifting with field, whereas the FM contribution increases rapidly and at 14 T only the FM state exists in the whole temperature range.

As the magnetic field of 14 T stabilizes the FM state in the whole temperature range, this field should be sufficient to initiate the AF-FM transition even at low temperature. Therefore, we attempted to investigate the peculiarities of this metamagnetic transition down to the lowest available temperature, $T = 2$ K. In Fig. 8(a), among $M(H)$ dependences measured at different temperatures, of particular interest are those below 10 K where the metamagnetic transition occurs in very distinctive jumps, being most prominent at 2 K (see Fig. 8 magnified in the region of the AF-FM transition in Fig. 3 in the Supplemental Material [25]). Similar phenomena have been reported earlier [22,33] and are often observed at very low temperature (2–10 K) where the kinetics of the magnetic phase transition can change. Low temperature ultrasharp magnetization steps have already been observed in manganites [34,35], $LaFe_{12}B_6$ [36], and single-crystalline $(Mn, Co)_2Sb$ [37]. Furthermore, similar magnetization jumps have been found also in permanent magnets [38–40]. Some authors attributed such jumps to significant thermal instabilities due to a small lattice specific heat at low temperature [38,39]; others suggested that the anomalies are caused by a quantum tunneling of the domain wall through the intergrain boundary [40].

In order to investigate if these jumps might be a result of thermal instabilities, for $M(H)$ at 2 K various field sweep rates were employed [see Fig. 8(b)]. The occurrence of the rectangular jumps was not affected, with the exception of the sweep rate of 0.01 T/s; then the curve looks smoother, which can be due to the time resolution of the measurement. This excludes the idea of the thermal instabilities' effect during the measurement; with a slower rate, the staircase behavior becomes only more distinct. The origin of this is not well understood. As a hypothesis, it may be related to the AF-FM phase boundary motion that is pinned by defects or inhibited by the stray field of the parts that have already transformed.

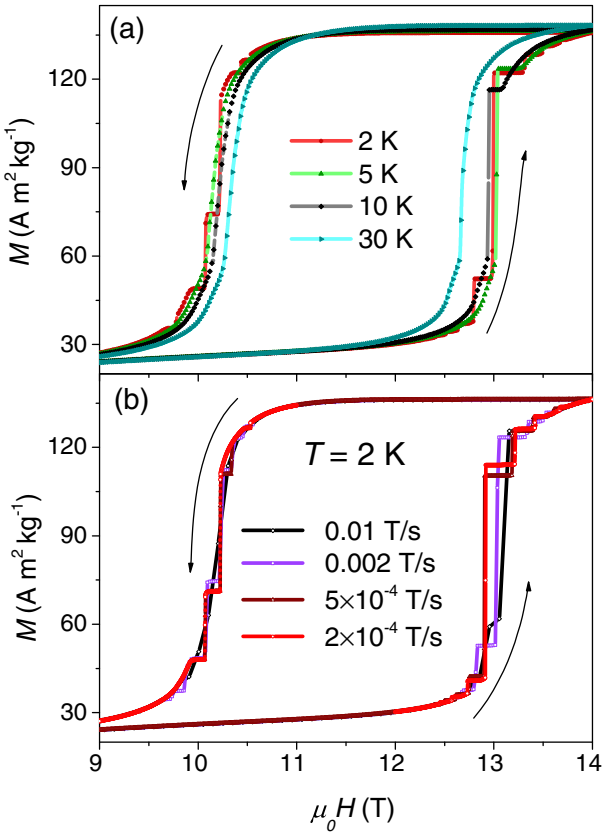


FIG. 8. (a) Field dependences of the magnetization of Ni-doped FeRh measured in the range of 2–30 K. The staircase behavior of the magnetization is observed below 10 K. (b) field dependences of the magnetization at 2 K measured at different field sweep rates.

Then, upon the further increase of the magnetic field, the advance of the phase boundary will occur in an avalanchelike fashion.

Furthermore, in order to study the dynamics of the metamagnetic transition in FeRh, magnetization measurements have been carried out using (1) a quasistatic magnetic field in a superconducting magnet with a field sweeping rate of $5 \times 10^{-3}$ T/s and (2) a pulsed magnetic field with a field sweeping rate $\sim 10^3$ T/s. These measurements correspond to isothermal and adiabatic conditions, respectively. The field dependences are shown in Fig. 9 (see more graphs at other temperatures in Fig. 2 in the Supplemental Material [25]). In a pulsed field, the hysteresis loop is broader and has an asymmetrical shape. The mechanism of broadening of the hysteresis in a pulsed field is not completely clear; possibly, at a faster sweep rate the lattice that participates in the transition with a volume expansion of 1% [41] requires more time to complete the process.

Earlier, magnetization in a pulsed field and static field has been compared for $La(Fe, Si, Co)_{13}$ [32]: In a pulsed field the metamagnetic transition was shifted towards higher fields, due to the heating of the sample under adiabatic conditions because of the conventional magnetocaloric effect. In the case of FeRh and the inverse MCE, it is difficult to relate the adiabatic and isothermal $M(H)$ in a similar way. Applied to this AF-FM transition, it could explain the shift of the transition towards

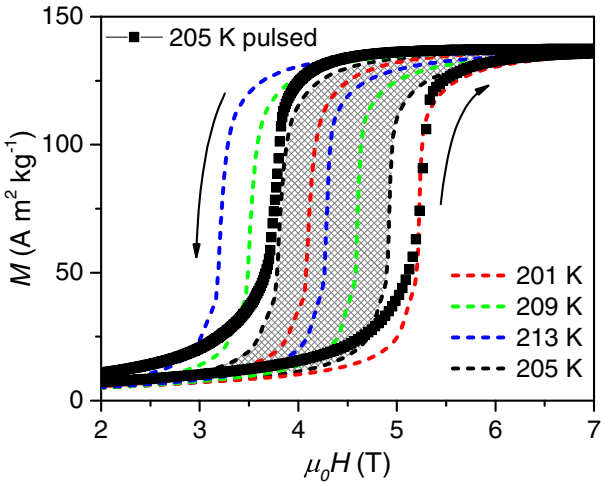


FIG. 9. Field dependence of the magnetization measured under adiabatic conditions in pulsed fields ($\sim 10^3$ T/s, black stars) and under isothermal conditions in quasistatic fields ($\sim 10^3$ T/s, dashed lines; the respective hysteresis area is hashed). See the Supplemental Material [25] for more graphs.

higher field in a pulsed field due to the MCE and cooling of the sample. However, the FM-AF transition is shifted to lower fields, broadening the hysteresis, which means overheating of the sample. Therefore, there must additionally be another mechanism in place.

The overheating during pulsed field application has been, in fact, observed during the direct measurements of $\Delta T_{ad}$ (in Fig. 5). The temperature rise between the starting and final points was compared to the irreversible hysteresis losses that could be expected based on the area of the magnetization loop obtained also in the pulsed magnetic field at these temperatures (see Fig. 9 and the Supplemental Material [25]) and respective heat capacity. The area of the magnetization loop reflects the dissipation energy for the magnetically irreversible process: $W = Q = \oint_{\text{cycle}} H dM$, and the respective temperature change is $\Delta T_{\text{cycle}} = Q/(C_{H,P})$. It has been proposed earlier [22] that the change of the temperature at the magnetostructural transition in FeRh can be due to two mechanisms: (1) the magnetocaloric effect due to the entropy change and (2) an irreversible heating due to the propagation of the wall between the AF and FM phases. The first mechanism should be more prominent at high temperatures, and the second one at low temperatures, as we indeed observe here. In order to provide more experimental evidence on this matter, we measured field dependences of magnetization at 5.7 K, where according to our data (Fig. 6) the MCE is not expected at the AF-FM transition. The additional Cernox thermometer was attached directly to the sample in order to monitor the temperature of the sample during the magnetization-demagnetization process. The result of these measurements is shown in Fig. 10(b). In the near-isothermal conditions, there is a heating of the sample by 2 K during both AF-FM and FM-AF transitions. Since at low temperatures the magnetic entropy change is almost zero and the Ni-doped FeRh does not have a magnetocaloric effect, the thermal effect shown in Fig. 10 must be related exclusively to magnetic hysteresis and dissipation losses.

Using field and temperature dependences of the magnetization, a magnetic phase diagram was constructed (see Fig. 11). The diagram marks the regions where only the AF and FM states exist, as well as their mixed state which corresponds to the hysteresis. The red symbols indicate the transition from the AF to the FM state, the blue symbols indicate the reverse FM-AF transition; the hashed region in between is the hysteresis. Usually, the average critical field in this case is fitted using a quadratic dependence [22,23]. When a deviation from it in the high temperature region is observed, it is ascribed to the magnetocaloric effect [37]. The broadening of the hysteresis in FeRh towards low temperatures can be affected, on one hand, by the characteristics of the electronic structure according to the thermal activation model and, on the other hand, by magnetoelastic interactions [22]. "Freezing" of $dT/dH$ approaching low temperatures can be addressed from the point of the arrest of the phase transition kinetics [42,43] and competition of the magnetic and lattice entropy in inverse magnetocaloric materials [44].

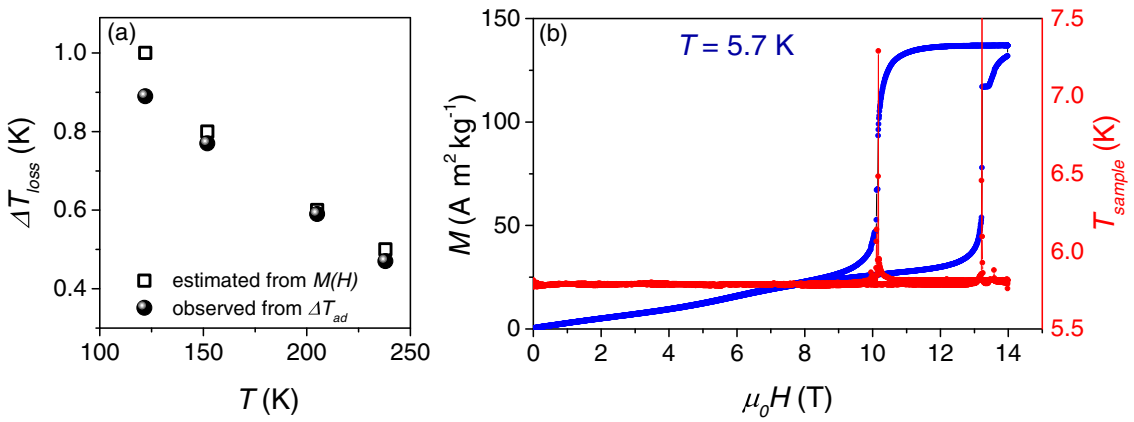


FIG. 10. (a) Estimation of the expected losses from adiabatic $M(H)$ loops compared to the overheating obtained during the direct measurements of $\Delta T_{ad}$ in a 14 T pulsed field. (b) $M(H)$ dependence measured in a Quantum Design PPMS at 5.7 K measured by an additional thermometer attached directly to the sample.

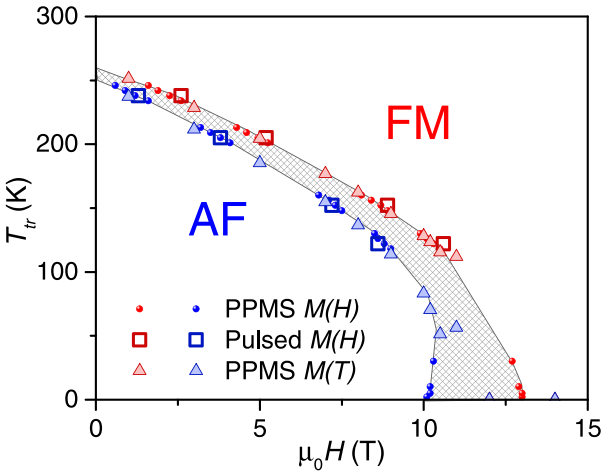


FIG. 11. Magnetic phase diagram: Red symbols mark the transition occurring on the field/temperature increase, and blue, on the decrease. Respective AF and FM areas are marked, and the hysteresis area is hashed as a guide to the eye.

## IV. CONCLUSION

Direct measurements of the adiabatic temperature change carried out in pulsed fields for Ni-doped FeRh have shown excellent agreement with direct measurements at slower field sweep rates, made using a Halbach setup, as well as with the estimation made from the *S-T* diagram built using heat capacity measurements. The maximal $\Delta T_{ad}$ in Ni-doped FeRh obtained in the discontinuous mode is −7.4 K in a 2 T magnetic field, while the cyclic value is −4.6 K. The $\Delta T_{ad}$ in Ni-doped $Fe_{49}Rh_{51}$ is reduced compared to that of the binary compound [19]; however, this effect was less for the cyclic value, which means that the modified compound with a tuned transition temperature will retain the high MCE value at the level of benchmark material (Gd), under cyclic conditions as well. The measurements carried out in high magnetic field of 14 T revealed that the MCE in Ni-doped FeRh saturates and does not change further upon the field increase. The observed effects demonstrate that magnetic refrigerants of the nature comparable to FeRh would be most efficient in magnetic fields up to 2 T, but not in high fields.

The sample temperature after the applied pulsed field and completed transformation does not return to the original temperature, showing an overheating up to 1 K and by estimation, coincides with the hysteresis losses estimated from $M(H)$ dependences. This effect increases towards low temperatures and may be common for all FeRh-based alloys. The metamagnetic transition in pulsed fields with the rate $10^3$ T/s has a broader hysteresis than in a magnetic field with the slow rate of $10^{-3}$ T/s. At $T = 2$ K and even slower rate of $10^{-4}$ T/s the AF-FM transition occurs in a staircase manner. The magnetic phase diagram shows a close to linear shift of the transition field at high temperatures and a freezing of that shift towards low temperatures which is usually described by a quadratic dependence and most likely is due to the counteracting of the lattice and magnetic contributions in the entropy change as in other inverse magnetocaloric materials [44].

## ACKNOWLEDGMENTS

We acknowledge the support of the HLD-HZDR, member of the European Magnetic Field Laboratory (EMFL); TU Darmstadt acknowledges funding from the European Research Council (ERC) under the European Union's Horizon 2020 research and innovation program (Grant No. 743116—project Cool Innov) and the Deutsche Forschungsgemeinschaft (DFG, German Research Foundation), Project ID No. 405553726-TRR 270, Germany. Ural Federal University acknowledges the support by Act 211 Government of the Russian Federation, Contract No. 02.A03.21.0006; A.Y.K. gratefully acknowledges the financial support of the Ministry of Science and Higher Education of the Russian Federation in the framework of Increase Competitiveness Program of MISiS (Grant No. P02 2017-2-6). N.V.B. acknowledges support by the Ministry of Science and Higher Education of the Russian Federation (Theme No. AAAA-A18-118020290129-5).

[1] I. Takeuchi and K. Sandeman, Phys. Today **68**(12), 48 (2015).
[2] V. Franco, J. Blázquez, B. Ingale, and A. Conde, Annu. Rev. Mater. Res. **42**, 305 (2012).
[3] V. Franco, J. S. Blázquez, J. J. Ipus, J. Y. Law, L. M. Moreno-Ramírez, and A. Conde, Prog. Mater. Sci. **93**, 112 (2018).
[4] K. G. Sandeman, Scr. Mater. **67**, 566 (2012).
[5] A. Kitanovski, Adv. Energy Mater. **10**, 1903741 (2020).
[6] V. K. Pecharsky and K. A. Gschneidner Jr., Phys. Rev. Lett. **78**, 4494 (1997).
[7] O. Gutfleisch, M. A. Willard, E. Brück, C. H. Chen, S. G. Sankar, and J. P. Liu, Adv. Mater. **23**, 821 (2011).
[8] V. Chaudhary, X. Chen, and R. V. Ramanujan, Prog. Mater. Sci. **100**, 64 (2019).
[9] E. Brück, O. Tegus, D. T. Cam Thanh, N. T. Trung, and K. H. J. Buschow, Int. J. Refrig. **31**, 763 (2008).
[10] K. P. Skokov, V. V Khovaylo, K.-H. Müller, J. D. Moore, J. Liu, and O. Gutfleisch, J. Appl. Phys. **111**, 07A910 (2012).
[11] T. Gottschall, K. P. Skokov, B. Frincu, and O. Gutfleisch, Appl. Phys. Lett. **106**, 021901 (2015).
[12] T. Gottschall, K. P. Skokov, M. Fries, A. Taubel, I. Radulov, F. Scheibel, D. Benke, S. Riegg, and O. Gutfleisch, Adv. Energy Mater. **9**, 1901322 (2019).
[13] F. Scheibel, T. Gottschall, A. Taubel, M. Fries, K. P. Skokov, A. Terwey, W. Keune, K. Ollefs, H. Wende, M. Farle, M. Acet, O. Gutfleisch, and M. E. Gruner, Energy Technol. **6**, 1397 (2018).
[14] O. Gutfleisch, T. Gottschall, M. Fries, D. Benke, I. Radulov, K. P. Skokov, H. Wende, M. Gruner, M. Acet, P. Entel, and M. Farle, Philos. Trans. R. Soc., A **374**, 20150308 (2016).
[15] T. Gottschall, K. P. Skokov, F. Scheibel, M. Acet, M. Ghorbani Zavareh, Y. Skourski, J. Wosnitza, M. Farle, and O. Gutfleisch, Phys. Rev. Appl. **5**, 024013 (2016).
[16] F. Scheibel, T. Gottschall, K. Skokov, O. Gutfleisch, M. Ghorbani-Zavareh, Y. Skourski, J. Wosnitza, Ö. Çakır, M. Farle, and M. Acet, J. Appl. Phys. **117**, 233902 (2015).

[17] S. A. Nikitin, G. Myalikgulyev, A. M. Tishin, M. P. Annaorazov, K. A. Asatryan, and A. L. Tyurin, Phys. Lett. A **148**, 363 (1990).
[18] J. Liu, T. Gottschall, K. P. Skokov, J. D. Moore, and O. Gutfleisch, Nat. Mater. **11**, 620 (2012).
[19] A. Chirkova, K. P. Skokov, L. Schultz, N. V. Baranov, O. Gutfleisch, and T. G. Woodcock, Acta Mater. **106**, 15 (2016).
[20] E. Stern-Taulats, A. Gràcia-Condal, A. Planes, P. Lloveras, M. Barrio, J.-L. Tamarit, S. Pramanick, S. Majumdar, and L. Mañosa, Appl. Phys. Lett. **107**, 152409 (2015).
[21] S. Yuasa, Y. Otani, H. Miyajima, and A. Sakuma, IEEE Transl. J. Magn. Jpn. **9**, 202 (1994).
[22] N. V. Baranov and E. A. Barabanova, J. Alloys Compd. **219**, 139 (1995).
[23] J. B. McKinnon, D. Melville, and E. W. Lee, J. Phys. C: Solid State Phys. **3**, S46 (1970).
[24] L. H. Lewis, C. H. Marrows, and S. Langridge, J. Phys. D: Appl. Phys. **49**, 323002 (2016).
[25] See Supplemental Material at http://link.aps.org/supplemental/10.1103/PhysRevMaterials.5.064412 for the structural characterization of the sample [XRD and scanning electron microscopy (SEM)], additional measurements of adiabatic and isothermal $M(H)$ at different temperatures, and an enlarged region near the field-driven AF-FM transition at low temperatures.
[26] A. Chirkova, F. Bittner, K. Nenkov, N. V. Baranov, L. Schultz, K. Nielsch, and T. G. Woodcock, Acta Mater. **131**, 31 (2017).
[27] J. Wosnitza, A. D. Bianchi, J. Freudenberger, J. Haase, T. Herrmannsdörfer, N. Kozlova, L. Schultz, Y. Skourski, S. Zherlitsyn, and S. A. Zvyagin, J. Magn. Magn. Mater. **310**, 2728 (2007).
[28] M. Ghorbani Zavareh, C. Salazar Mejía, A. K. Nayak, Y. Skourski, J. Wosnitza, C. Felser, and M. Nicklas, Appl. Phys. Lett. **106**, 071904 (2015).
[29] V. K. Pecharsky and K. A. Gschneidner, J. Appl. Phys. **86**, 565 (1999).
[30] E. Stern-Taulats, A. Planes, P. Lloveras, M. Barrio, J.-L. Tamarit, S. Pramanick, S. Majumdar, C. Frontera, and L. Mañosa, Phys. Rev. B **89**, 214105 (2014).
[31] A. P. Kamantsev, A. A. Amirov, Y. S. Koshkid'ko, C. S. Mejía, A. V. Mashirov, A. M. Aliev, V. V. Koledov, and V. G. Shavrov, Phys. Solid State **62**, 160 (2020).
[32] M. G. Zavareh, Y. Skourski, K. P. Skokov, D. Y. Karpenkov, L. Zvyagina, A. Waske, D. Haskel, M. Zhernenkov, J. Wosnitza, and O. Gutfleisch, Phys. Rev. Appl. **8**, 014037 (2017).
[33] E. Baranov, N. V. Sinitsyn, E. V. Kozlov, and A. I. Barabanova, Fiz. Met. Metalloved. **2**, 100 (1991).
[34] V. Hardy, S. Majumdar, M. R. Lees, D. M. Paul, C. Yaicle, and M. Hervieu, Phys. Rev. B **70**, 104423 (2004).
[35] R. Mahendiran, A. Maignan, S. Hébert, C. Martin, M. Hervieu, B. Raveau, J. F. Mitchell, and P. Schiffer, Phys. Rev. Lett. **89**, 286602 (2002).
[36] L. V. B. Diop and O. Isnard, Appl. Phys. Lett. **108**, 132401 (2016).
[37] M. I. Bartashevich, T. Goto, T. Tomita, N. V. Baranov, S. V. Zemlyanski, G. Hilscher, and H. Michor, Phys. B (Amsterdam, Neth.) **318**, 198 (2002).
[38] A. Handstein, D. Eckert, K.-H. Muller, B. Wall, and W. Rodewald, IEEE Trans. Magn. **30**, 598 (1994).
[39] D. S. Neznakhin, A. S. Bolyachkin, A. S. Volegov, P. E. Markin, S. V. Andreev, and N. V. Kudrevatykh, J. Magn. Magn. Mater. **377**, 477 (2015).
[40] N. V. Baranov, E. V. Sinitsyn, E. A. Ignatyev, and S. V. Andreev, J. Magn. Magn. Mater. **130**, 133 (1994).
[41] A. I. Zakharov, A. M. Kadomtseva, P. Z. Levitin, and E. G. Ponyatovskii, Zh. Eksp. Teor. Fiz. **46**, 2003 (1964) [JETP **19**, 1348 (1964)].
[42] M. Manekar, M. K. Chattopadhyay, and S. B. Roy, J. Phys.: Condens. Matter **23**, 086001 (2011).
[43] M. K. Chattopadhyay, K. Morrison, A. Dupas, V. K. Sharma, L. S. Sharath Chandra, L. F. Cohen, and S. B. Roy, J. Appl. Phys. **111**, 053908 (2012).
[44] T. Gottschall, K. P. Skokov, D. Benke, M. E. Gruner, and O. Gutfleisch, Phys. Rev. B Phys. **93**, 184431 (2016).